Original Article

Clinical value of quantitative analysis of contrast-enhanced ultrasonography in the differential diagnosis of benign and malignant pelvic tumors

Qiyun Fan, Yin Zhang, Fa Wang, Hui Chen, Qianru Xie, Bing Ji, Ting Qiu, Weihui Shentu, Hongying Wang, Yingheng Wu

Department of Medical Ultrasonics, Guangzhou Women and Children's Medical Center, Guangzhou Medical University, Guangzhou, China

Contributions: (I) Conception and design: Q Fan, W Shentu, Y Wu; (II) Administrative support: H Wang; (III) Provision of study materials or patients: Q Fan, W Shentu, H Chen, B Ji, T Qiu; (IV) Collection and assembly of data: Y Zhang, Y Wu, Q Xie; (V) Data analysis and interpretation: Q Fan, Y Zhang; (VI) Manuscript writing: All authors; (VII) Final approval of manuscript: All authors.

Correspondence to: Yingheng Wu, MD; Weihui Shentu, PhD; Hongying Wang, PhD. Department of Medical Ultrasonics, Guangzhou Women and Children's Medical Center, Guangzhou Medical University, No. 402, Renmin Zhong Road, Guangzhou 510182, China. Email: 49408497@qq.com; shentuwh@gwcmc.org; why0118@163.com.

Background: Cervical cancer, endometrial cancer, and ovarian cancer are among the top 10 most common cancers in women, with ovarian cancer in particular being considered a "silent killer". Therefore, early detection, diagnosis, and treatment constitute important means of care for women's health. This study investigated the clinical value of the quantitative analysis of contrast-enhanced ultrasonography (CEUS) in the differential diagnosis of benign and malignant pelvic tumors.

Methods: CEUS was performed on 151 patients with pelvic masses. Subsequently, a qualitative diagnosis was completed using the image enhancement features and tumor parameters. A multiparametric analysis of CEUS images was performed, which included the following parameters: arrival time (AT), time to peak (TTP), peak intensity (PI), and ascent slope (AS). In addition, the qualitative diagnostic efficiency of CEUS was assessed in a multiparametric analysis, and the results were compared with pathological findings.

Results: The patients in the malignant group were older (P=0.001) and had larger lesion PI values (P<0.01) than those in the benign group. The PI difference (PI_d) and the AS difference (AS_d) showed statistical differences (P<0.01) between the myometrium and lesion tissues in the same patient. Moreover, the PI_d and AS_d showed the largest receiver operating characteristic (ROC) curve and area under the ROC curve (AUC), with sensitivities of 90.9% and 91.7% and specificities of 86.4% and 72.5%, respectively.

Conclusions: The quantitative analysis of CEUS provides a new, simpler, and more accurate method for the differential diagnosis of benign and malignant pelvic masses in clinical practice. The sensitivities and specificities of PId and ASd were higher compared to other parameters from the same patient.

Keywords: Contrast-enhanced ultrasonography (CEUS); pelvic mass; parameters; quantitative analysis; clinical practice

Introduction

Among pelvic tumors, cervical cancer, endometrial cancer, and ovarian cancer are among the top 10 most common cancers in women (1). Among these, ovarian cancer is considered to be a "silent killer", as most patients present with few symptoms or are diagnosed at the advanced stages (III and IV) (2,3). Consequently, early detection, diagnosis, and treatment are critical to in the management of this disease and women's health generally. Traditional ultrasonography and Doppler ultrasonography have limited use in examining smaller lesions, and improving the early diagnosis of malignancy is pivotal to enhancing the efficacy of treatment.

Contrast-enhanced ultrasonography (CEUS) has been widely applied in the diagnosis of liver, thyroid, breast, and renal diseases, and its diagnostic value for tumors has been consistently recognized (4-7) due to its high sensitivity and specificity. However, only a few studies thus far have conducted qualitative or quantitative analyses of the differential diagnosis of pelvic tumors. Furthermore, there is a crossover of quantitative indices in benign and malignant lesions and a lack of a uniform standard for each index (8,9). Qualitative analysis is also susceptible to considerable subjective and operational differences, which limits its clinical application (10). In this study, a comprehensive quantitative analysis of multiple indicators in identifying benign and malignant pelvic tumor lesions was conducted. Overall, the findings of this study have the potential to improve the diagnostic accuracy of CEUS and may serve as a more reliable reference for the clinical management of tumors. We present this article in accordance with the STARD reporting checklist (available at https://qims.amegroups.com/article/view/10.21037/qims-23-582/rc).

Methods

Sample sources

This study retrospectively reviewed a total of 155 patients admitted to Guangzhou Women and Children's Medical Center for pelvic tumors between April 2021 and September 2022. The study was conducted in accordance with the Declaration of Helsinki (as revised in 2013) and was approved by ethics committee of Guangzhou Women and Children's Medical Center (No. 194A01). Informed consent was obtained from all patients.

Inclusion criteria

The inclusion criteria of patients were as follows: (I) a pelvic tumor detected with general ultrasonography; (II) a pelvic tumor confirmed via surgery and biopsy; (III) a negative urine pregnancy test result; and (IV) no contraindications to imaging, such as severe allergy, severe cardiopulmonary system disease, pregnancy, or lactation. In addition, junctional lesions and hyperplastic active lesions were classified as malignant tumors to facilitate statistical analysis.

Equipment and methods

Equipment

The Mindray Resona 70B Diasonograph (probe model: SC5-1U and V11-3HU; Mindray Company, Shenzhen, China) was used as the examination apparatus in this study. CEUS was performed using cadence-contrast pulse sequencing (CPS) imaging technology. To reduce microbubble destruction, the machine parameters were set to the following: acoustic power (AP), 1.29%; mechanical index (MI), 0.082; frequency (F), 2.2; frame rate (FR), 9; and dynamic range (DR), 105.

Contrast agent

The ultrasound contrast agent SonoVue (Bracco, Milan, Italy) was used and prepared as follows: 1.5 mL for a single transabdominal examination and 2.4 mL for a single transvaginal examination through the antecubital vein.

Conventional ultrasonography and CEUS imaging

Transabdominal ultrasonography and transvaginal ultrasonography were performed, and the location, size, borders, internal echogenicity, blood flow, spectral pattern, and resistance index of the lesion were recorded. The imaging mode was then switched to the contrast imaging mode. The specific location of the lesion was used to decide the type of examination (transabdominal CEUS or transvaginal CEUS), with the lesion placed in the center of the image and the focus adjusted to the base level of the lesion. The image depth was adjusted to 8–12 cm according to the location of the pelvic mass. Time gain compensation was adjusted to achieve a homogeneous signal intensity of the mass. All settings were kept constant throughout each examination. The time of contrast agent injection was also recorded. The enhancement of the lesion and its surrounding tissue and its dynamic course were monitored
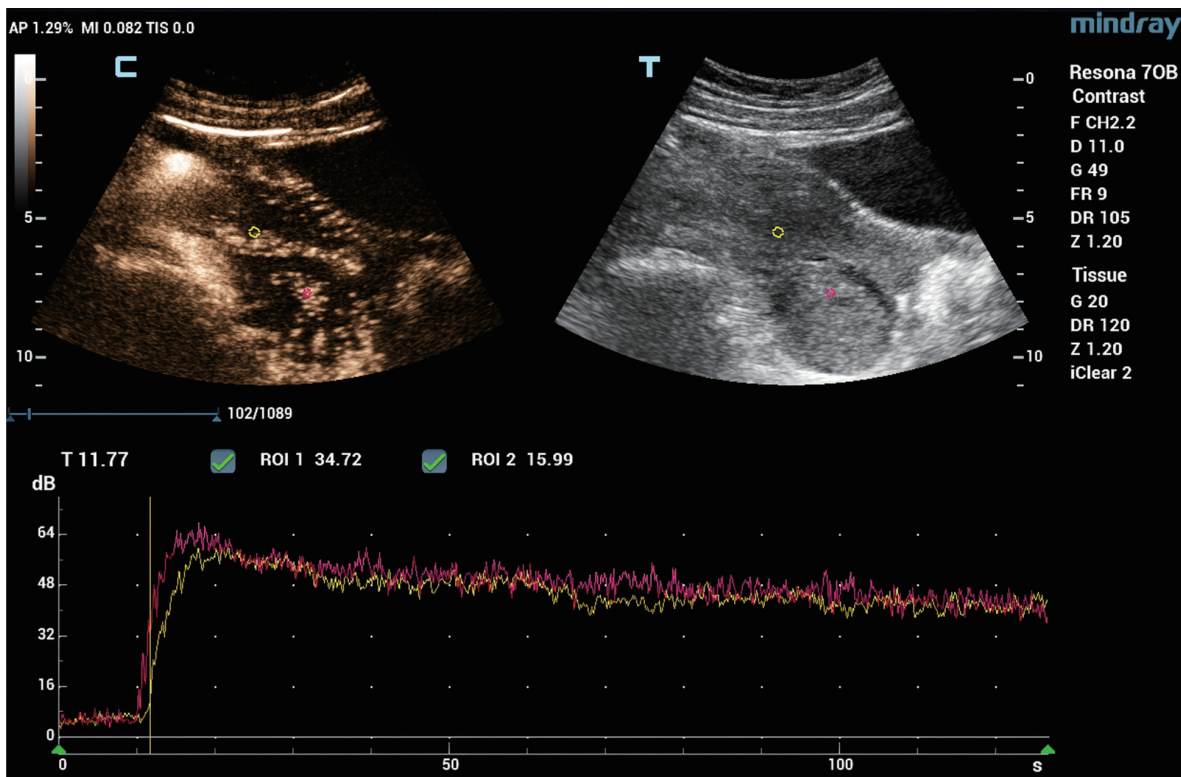
Figure 1 The ROI was plotted for the myometrium (yellow circle) and lesion (pink circle) to obtain the TIC of the ROI (horizontal coordinate: time; longitudinal coordinate: PI). AP, acoustic power; MI, mechanical index; TIS, tissue; C, contrast; T, tissue; F, frequency; D, depth; G, gain; FR, frame rate; DR, dynamic range; Z, zoom; T 11.77, time 11.77; ROI, region of interest; dB, decibel; TIC, time-intensity curve; PI, peak intensity.

in real time. Finally, the imaging data obtained from the CEUS process were saved. The target lesion was observed continuously for 2–3 minutes.

Image analysis

The CEUS images were analyzed two physicians with more than 5 years of experience in ultrasonic diagnosis. The time, level, pattern, and mode of enhancement were observed and recorded for the lesions. Based on the myometrium profile, the enhancement time of the lesion was categorized into early, simultaneous, and late. The enhancement pattern was categorized into uniform and nonuniform, while the enhancement level was categorized into high, intermediate, low, and no enhancement. An automatic machine quantitative analysis software was used to draw a region of interest (ROI) for each myometrium and lesion as well as to obtain the time-intensity curve (TIC) for the ROI (*Figure 1*). Data with goodness of fit (GOF) >0.8 were selected to record the contrast arrival time (AT), time to

peak (TTP), peak intensity (PI), and ascent slope (AS) for the myometrium and the lesion (*Figure 2*). Subsequently, the AT difference (AT_d), the PI difference (PI_d), and the AS difference (AS_d) between the corrected myometrium and the lesion of the same patient were calculated as follows:

$$AT_d = \text{lesion AT} - \text{myometrium AT} \qquad [1]$$

$$PI_d = \text{lesion PI} - \text{myometrium PI} \qquad [2]$$

$$AS_d = \text{lesion AS} - \text{myometrium AS} \qquad [3]$$

Statistical analysis

The SPSS version 26 (SPSS Inc., Chicago, IL, USA) was used to perform data analysis. Quantitative data are expressed as mean ± standard deviation (SD). The independent samples *t*-test was used where P<0.01 was considered statistically significant. The cutoff values for the benignity and malignancy of each index were determined using receiver operating characteristic (ROC) curves.
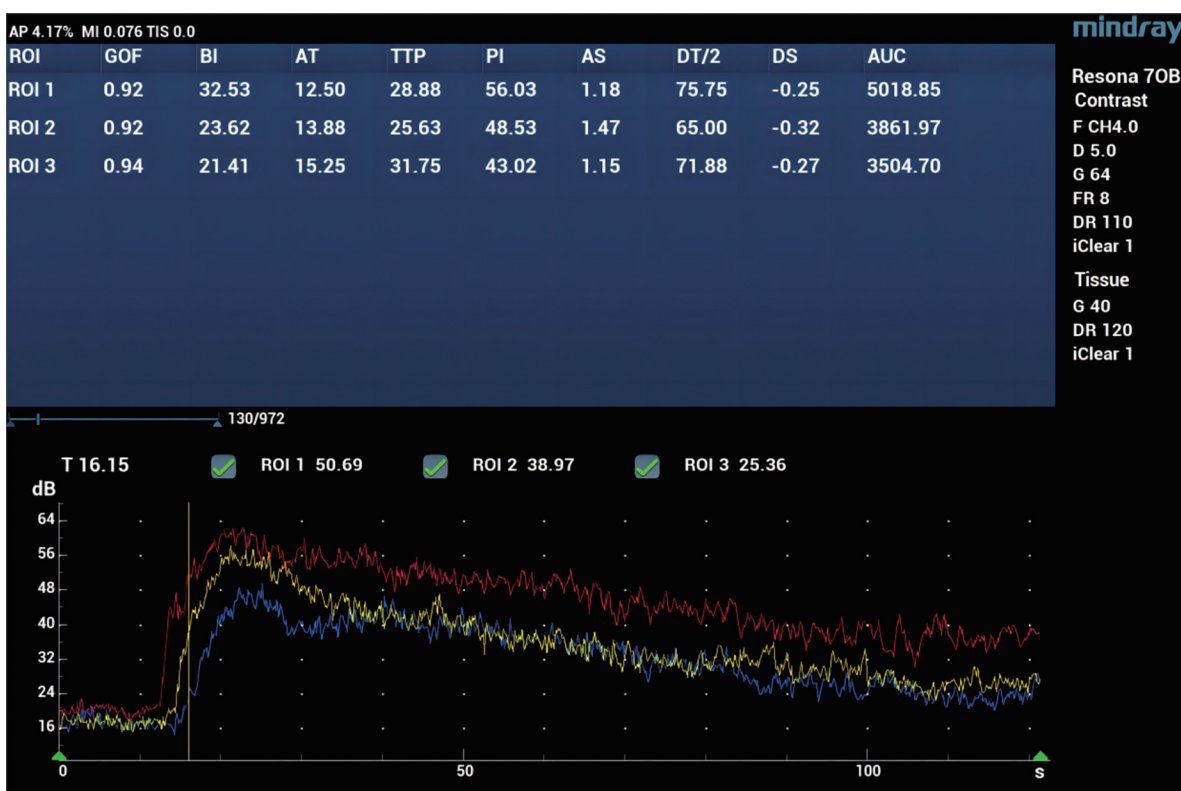
Figure 2 The data after the TIC of the ROI was obtained, with data with GOF >0.8 being selected (horizontal coordinate: time; longitudinal coordinate: PI). AP, acoustic power; MI, mechanical index; TIS, tissue; ROI, region of interest; GOF, goodness of fit; BI, base intensity; AT, arrival time; TTP, time to peak; PI, peak intensity; AS, ascending slope; DT, descending time; DS, descending slope; AUC, area under TIC (Mindray Company); TIC, time-intensity curve; F, frequency; D, depth; G, gain; FR, frame rate; DR, dynamic range; T, time; dB, decibel.

Results

From April 2021 to September 2022, 155 patients with pelvic tumors who underwent conventional transabdominal or transvaginal ultrasonography examination in Guangzhou Women and Children's Medical Center were recruited. The flowchart for patient selection is illustrated in *Figure 3*. There were 3 pregnant patients, 1 patient with atrial septal defect, and 20 patients who did not have any pathological findings who were excluded from the study. Finally, a total of 131 patients were enrolled in this investigation, including 109 (83.2%) patients with benign lesions and 22 (16.8%) patients with malignant and junctional lesions. All the lesions underwent histological verification, and the characteristics are listed in *Table 1*.

All patients were females with a mean age of 39.21±0.96 (range, 19–72) years. The patients in the malignant group were older (46.32±10.48 *vs.* 37.78±10.50 years, P=0.001) and had larger lesion PI values (56.90±9.36 *vs.* 43.15±8.41, P<0.01) than did those in the benign group (*Table 2*).

The AT_d was significantly lower in the malignant group than in the benign group (−0.632±1.28 *vs.* 0.686±2.41 s, P=0.014). Moreover, the PI_d (13.569±12.21 *vs.* −7.003±8.77, P<0.01), AS (2.819±1.15 *vs.* 2.019±0.85, P=0.005), and AS_d (1.205±1.27 *vs.* −0.179±0.90, P<0.01) values were significantly higher in the malignant group than in the benign group (*Table 3*).

According to the ROC curve, the area under the ROC curve (AUC) value of the PI curve was 0.899, with a 95% confidence interval (CI) of 0.813–0.986. When the cutoff value was 51.59, the sensitivity and specificity reached
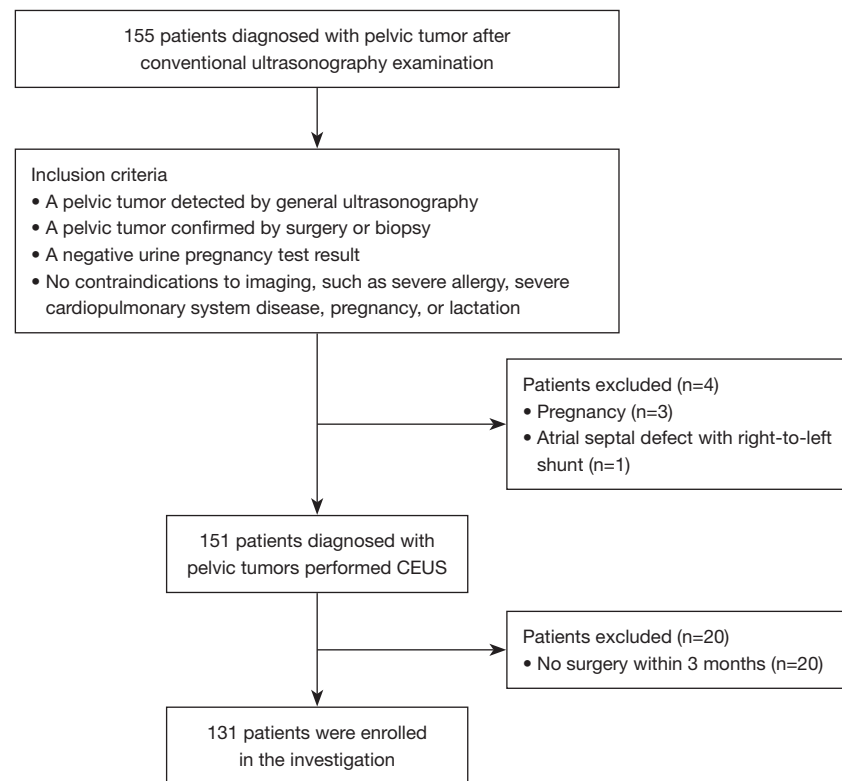
Figure 3 Flowchart for selection of patients with pelvic tumor. In total, 131 out of 155 patients were included according to the selection criteria. CEUS, contrast-enhanced ultrasonography.

Table 1 Pathological types of pelvic masses (n=131)

Pathological type	N (%)
Benign	109 (83.2)
Simple cyst	10 (7.6)
Mesosalpinx cyst	6 (4.6)
Mature teratoma	27 (20.6)
Hydrosalpinx	2 (1.6)
Serous cystadenoma	10 (7.6)
Fibrothecoma	5 (3.8)
Endometrioma	24 (18.3)
Brenner tumor	3 (2.3)
Endometrial polyp	7 (5.3)
Hysteromyoma	15 (11.5)

Table 1 (*continued*)

Table 1 (*continued*)

Pathological type	N (%)
Malignant	22 (16.8)
Serous cystadenocarcinoma	4 (3.0)
Mucinous cystadenocarcinoma	3 (2.3)
Endometroid adenocarcinoma	2 (1.6)
Granulosa cell tumor	2 (1.6)
Sertoli-Leydig cell tumor	1 (0.7)
Clear cell carcinoma	1 (0.7)
Borderline cystadenoma	4 (3.0)
Immature teratoma	2 (1.6)
Cervical carcinoma	3 (2.3)

Table 2 A comparison of each quantitative index of the benign and malignant pelvic masses between the myometrium and the lesion

Parameters	Benign mass (n=109)	Malignant mass (n=22)	P value
Age (years)	37.78±10.50	46.32±10.48	0.001
Myometrial AT (s)	4.82±7.33	3.39±6.78	0.398
Myometrial TTP (s)	29.20±9.66	30.07±10.43	0.702
Myometrial PI	50.15±6.90	43.33±12.32	<0.01
Lesion AT (s)	5.51±8.15	2.76±5.50	0.133
Lesion TTP (s)	29.84±12.41	26.03±13.15	0.196
Lesion PI	43.15±8.41	56.90±9.36	<0.01

Data are presented as mean ± SD. AT, arrival time; TTP, time to peak; PI, peak intensity; SD, standard deviation.

Table 3 A comparison of the changes in each quantitative index of the benign and malignant pelvic masses between the myometrium and the lesion

Parameters	Benign mass (n=109)	Malignant mass (n=22)	P value
AT_d (s)	0.686±2.41	−0.632±1.28	0.014
PI_d (dB)	−7.003±8.77	13.569±12.21	<0.01
Myometrial AS	2.198±0.67	1.829±0.90	0.028
Lesion AS	2.019±0.85	2.819±1.15	0.005
AS_d	−0.179±0.90	1.205±1.27	<0.01

Data are presented as mean ± SD. AT_d, arrival time difference; PI_d, peak intensity difference; AS, ascent slope; AS_d, ascent slope difference; SD, standard deviation.
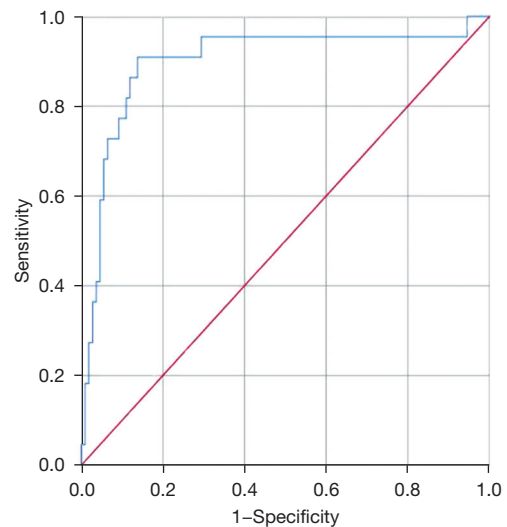

Figure 4 ROC curve for the lesion PI: AUC, 0.899; 95% CI, 0.813–0.986; cutoff value, 51.59; sensitivity, 90.9%; and specificity, 86.2%. ROC, receiver operating characteristic; PI, peak intensity; AUC, area under the ROC curve; CI, confidence interval.
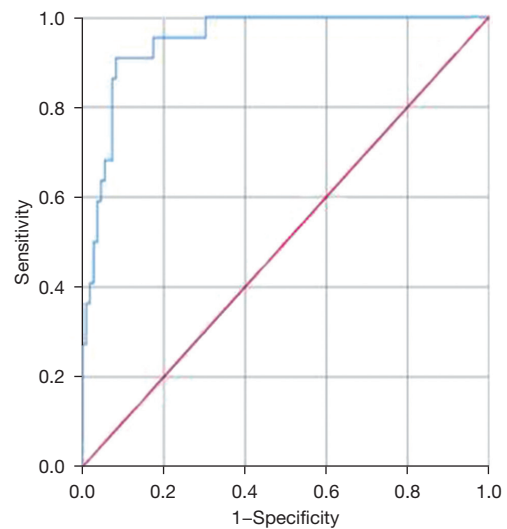

Figure 5 ROC curve for PId: AUC, 0.949; 95% CI, 0.911–0.987; cutoff value, 4.47; sensitivity, 90.9%; and specificity, 91.7%. ROC, receiver operating characteristic; PId, peak intensity difference; AUC, area under the ROC curve; CI, confidence interval.

90.9% and 86.2%, respectively (*Figure 4*). The AUC value of the PI_d curve was 0.949, with a 95% CI of 0.911–0.987. When the cutoff value was 4.47, the sensitivity and specificity were 90.9% and 91.7%, respectively (*Figure 5*). The AUC value of the AS curve of the lesion was 0.728, with a 95% CI of 0.606–0.851. When the cutoff value was 2.15, the sensitivity and specificity were 72.7% and 61.5%, respectively (*Figure 6*). The AUC value of the AS_d curve was 0.847, with a 95% CI of 0.763–0.930. When the cutoff value was 0.097, the sensitivity and specificity were 86.4% and 72.5%, respectively (*Figure 7*, *Table 4*).

Discussion

Currently, the common imaging methods for diagnosing pelvic masses are two-dimensional (2D) ultrasonography, computed tomography (CT), and magnetic resonance imaging (MRI), with ultrasound scores being used as a method of differentiation between benign and malignant
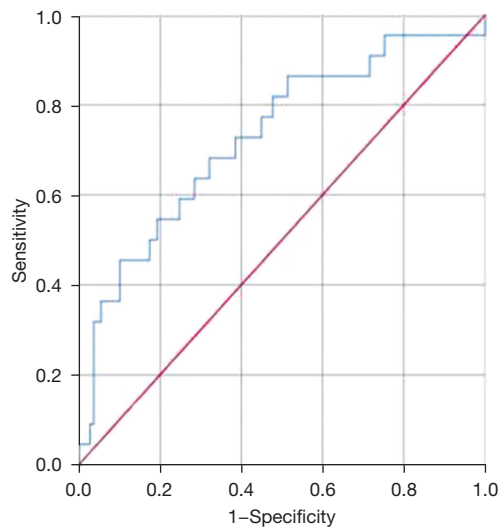
Figure 6 ROC curve for lesion AS: AUC, 0.728; 95% CI, 0.606–0.851; cutoff value, 2.15; sensitivity, 72.7%; and specificity, 61.5%. ROC, receiver operating characteristic; AS, ascent slope; AUC, area under the ROC curve; CI, confidence interval.
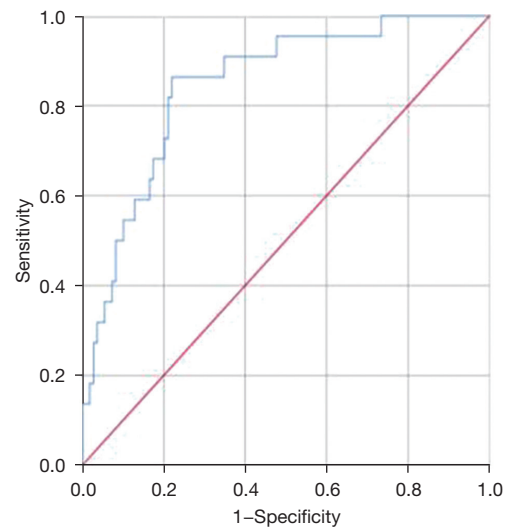

Figure 7 ROC curve for ASd: AUC, 0.847; 95% CI, 0.763–0.930; cutoff value, 0.097; sensitivity, 86.4%; and specificity, 72.5%. ROC, receiver operating characteristic; ASd, ascent slope difference; AUC, area under the ROC curve; CI, confidence interval.

Table 4 ROC curve analysis of the predicted probability of CEUS parameters for evaluation of benign and malignant pelvic tumor

Parameters	Sensitivity (%)	Specificity (%)	Cutoff value	AUC	95% CI	
					Lower limit	Upper limit
Lesion PI	90.9	86.2	51.59	0.899	0.813	0.986
PI_d	90.9	91.7	4.47	0.949	0.911	0.987
Lesion AS	72.7	61.5	2.15	0.728	0.606	0.851
AS_d	86.4	72.5	0.097	0.847	0.763	0.930

ROC, receiver operating characteristic; CEUS, contrast-enhanced ultrasonography; AUC, area under the ROC curve; CI, confidence interval; PI, peak intensity; PI_d, peak intensity difference; AS, ascent slope; AS_d, ascent slope difference.

masses (11,12). However, the use of CEUS in the diagnosis of pelvic masses has received little attention. CEUS allows for real-time dynamic observation of microcirculatory perfusion of the lesion. In addition, it uses software analysis and quantitative comprehensive evaluation of multiple indicators to improve the differential diagnosis of pelvic tumors based on their morphology and perfusion characteristics.

The phenomenon of neovascularization is quite commonly observed in pelvic malignant tumors. The lack of an intermediate muscular layer in new vessels causes low resistance. In addition, this neovascularization alters the amount and rate of blood perfusion, which manifests as a unique pathological angiogram of malignant tumors (13). Thus, this perfusion pattern of malignancy exhibits contrast perfusion preceding myometrial perfusion and hyperenhancement, which is consistent with previous findings (14-21). The uterine arteries originate from the internal iliac artery, and their main trunk divides bilaterally into superior and inferior branches at the level of internal ostium of the uterus. The superior branch of the uterine artery travels up along the lateral border of the uterus to its base, where it gives off branches and nourishes the uterus, fallopian tubes, and ovaries, and anastomoses with the

ovarian artery. This indicates that the perfusion patterns of the uterus and ovaries are similar in the event of the occurrence of a benign or malignant pelvic tumor.

In line with the findings of earlier research (22), the PI, AT_d, and AS values of the lesion in this study were all significantly higher in the malignant lesions than in benign lesions. Additionally, the myometrium was used as a reference in this study. Since blood perfusion is strongly influenced by individual differences in heart rate and vascular distribution, the parameters PI_d and AS_d were set to reduce any error arising due to these individual differences. The results demonstrated that the PI_d and AS_d values calculated for the same patient could effectively characterize the differences between benign and malignant tumors, with the PI_d and AS_d values being significantly higher in malignant tumors than in benign tumors. According to the generated ROC curves, when the PI_d cutoff value was 4.47, the sensitivity and specificity of PI_d were 90.9% and 91.7%, respectively. Moreover, when the AS_d cutoff value was 0.097, the sensitivity and specificity of AS_d were 86.4% and 72.5%, respectively. Both PI_d and AS_d had high sensitivity, specificity, positive predictive value, negative predictive value, and accuracy, along with the largest AUC value and the highest diagnostic efficacy. These findings suggest that CEUS has considerable clinical value for the qualitative diagnosis of malignant pelvic lesions.

There were certain limitations to this study. As we employed a single-center, retrospective design with a small number of cases, there might have been a bias in the selection of case types, especially for malignant tumors. Therefore, further prospective studies involving extensive data should be conducted. Continued investigation of pelvic masses that are challenging to characterize using conventional ultrasonography may improve the differential diagnosis and deliver more effective clinical assistance in the future.

Conclusions

A quantitative analysis of CEUS images can provide a novel, simple, and more accurate method for the differential diagnosis of benign and malignant pelvic masses in clinical practice. The sensitivity and specificity of both PI_d and AS_d were higher compared to other parameters in the same patient. Despite these findings, we believe that further studies are needed to evaluate the applicability of CEUS in the assessment of pelvic tumors.

Footnote

References

1. Berghuis AY, Pijnenborg JFA, Boltje TJ, Pijnenborg JMA. Sialic acids in gynecological cancer development and progression: Impact on diagnosis and treatment. Int J Cancer 2022;150:678-87.
2. Torre LA, Trabert B, DeSantis CE, Miller KD, Samimi G, Runowicz CD, Gaudet MM, Jemal A, Siegel RL. Ovarian cancer statistics, 2018. CA Cancer J Clin 2018;68:284-96.
3. Matulonis UA, Sood AK, Fallowfield L, Howitt BE, Sehouli J, Karlan BY. Ovarian cancer. Nat Rev Dis Primers

2016;2:16061.
4. Averkiou M, Powers J, Skyba D, Bruce M, Jensen S. Ultrasound contrast imaging research. Ultrasound Q 2003;19:27-37.
5. Liu H, Cao H, Chen L, Fang L, Liu Y, Zhan J, Diao X, Chen Y. The quantitative evaluation of contrast-enhanced ultrasound in the differentiation of small renal cell carcinoma subtypes and angiomyolipoma. Quant Imaging Med Surg 2022;12:106-18.
6. Jin H, Cai Y, Zhang M, Huang L, Bao W, Hu Q, Chen X, Zhou L, Ling W. LI-RADS LR-5 on contrast-enhanced ultrasonography has satisfactory diagnostic specificity for hepatocellular carcinoma: a systematic review and meta-analysis. Quant Imaging Med Surg 2023;13:957-69.
7. Zhu Y, Jia Y, Pang W, Duan Y, Chen K, Nie F. Ultrasound contrast-enhanced patterns of sentinel lymph nodes: predictive value for nodal status and metastatic burden in early breast cancer. Quant Imaging Med Surg 2023;13:160-70.
8. Zhou H, Sun J, Jiang T, Wu J, Li Q, Zhang C, Zhang Y, Cao J, Sun Y, Jiang Y, Liu Y, Zhou X, Huang P. A Nomogram Based on Combining Clinical Features and Contrast Enhanced Ultrasound LI-RADS Improves Prediction of Microvascular Invasion in Hepatocellular Carcinoma. Front Oncol 2021;11:699290.
9. Lu J, Zhou P, Jin C, Xu L, Zhu X, Lian Q, Gong X. Diagnostic Value of Contrast-Enhanced Ultrasonography With SonoVue in the Differentiation of Benign and Malignant Breast Lesions: A Meta-Analysis. Technol Cancer Res Treat 2020;19:1533033820971583.
10. Szymanski M, Socha MW, Kowalkowska ME, Zielińska IB, Eljaszewicz A, Szymanski W. Differentiating between benign and malignant adnexal lesions with contrast-enhanced transvaginal ultrasonography. Int J Gynaecol Obstet 2015;131:147-51.
11. Pelayo M, Pelayo-Delgado I, Sancho-Sauco J, Sanchez-Zurdo J, Abarca-Martinez L, Corraliza-Galán V, Martin-Gromaz C, Pablos-Antona MJ, Zurita-Calvo J, Alcázar JL. Comparison of Ultrasound Scores in Differentiating between Benign and Malignant Adnexal Masses. Diagnostics (Basel) 2023;13:1307.
12. Pelayo M, Sancho-Sauco J, Sanchez-Zurdo J, Abarca-Martinez L, Borrero-Gonzalez C, Sainz-Bueno JA, Alcazar JL, Pelayo-Delgado I. Ultrasound Features and Ultrasound Scores in the Differentiation between Benign and Malignant Adnexal Masses. Diagnostics (Basel)

2023;13:2152.
13. Delaney LJ, Machado P, Torkzaban M, Lyshchik A, Wessner CE, Kim C, Rosenblum N, Richard S, Wallace K, Forsberg F. Characterization of Adnexal Masses Using Contrast-Enhanced Subharmonic Imaging: A Pilot Study. J Ultrasound Med 2020;39:977-85.
14. Ordén MR, Jurvelin JS, Kirkinen PP. Kinetics of a US contrast agent in benign and malignant adnexal tumors. Radiology 2003;226:405-10.
15. Guerriero S, Alcazar JL, Coccia ME, Ajossa S, Scarselli G, Boi M, Gerada M, Melis GB. Complex pelvic mass as a target of evaluation of vessel distribution by color Doppler sonography for the diagnosis of adnexal malignancies: results of a multicenter European study. J Ultrasound Med 2002;21:1105-11.
16. Testa AC, Timmerman D, Van Belle V, Fruscella E, Van Holsbeke C, Savelli L, Ferrazzi E, Leone FP, Marret H, Tranquart F, Exacoustos C, Nazzaro G, Bokor D, Magri F, Van Huffel S, Ferrandina G, Valentin L. Intravenous contrast ultrasound examination using contrast-tuned imaging (CnTI) and the contrast medium SonoVue for discrimination between benign and malignant adnexal masses with solid components. Ultrasound Obstet Gynecol 2009;34:699-710.
17. Marret H, Sauget S, Giraudeau B, Brewer M, Ranger-Moore J, Body G, Tranquart F. Contrast-enhanced sonography helps in discrimination of benign from malignant adnexal masses. J Ultrasound Med 2004;23:1629-39; quiz 1641-42.
18. Testa AC, Timmerman D, Exacoustos C, Fruscella E, Van Holsbeke C, Bokor D, Arduini D, Scambia G, Ferrandina G. The role of CnTI-SonoVue in the diagnosis of ovarian masses with papillary projections: a preliminary study. Ultrasound Obstet Gynecol 2007;29:512-6.
19. Stoelinga B, Juffermans L, Dooper A, de Lange M, Hehenkamp W, Van den Bosch T, Huirne J. Contrast-Enhanced Ultrasound Imaging of Uterine Disorders: A Systematic Review. Ultrason Imaging 2021;43:239-52.
20. Xu J, Huang Z, Zeng J, Zheng Z, Cao J, Su M, Zhang X. Value of Contrast-Enhanced Ultrasound Parameters in the Evaluation of Adnexal Masses with Ovarian-Adnexal Reporting and Data System Ultrasound. Ultrasound Med Biol 2023;49:1527-34.
21. Hottat NA, Badr DA, Van Pachterbeke C, Vanden Houte K, Denolin V, Jani JC, Cannie MM. Added Value of Quantitative Analysis of Diffusion-Weighted

Imaging in Ovarian-Adnexal Reporting and Data System Magnetic Resonance Imaging 2022;56:158-70.

22. Shentu W, Zhang Y, Gu J, Wang F, Zhao W, Liu C, Lin Z, Wang Y, Liu C, Chen Y, Fan Q, Wang H. Contrast-enhanced ultrasonography for differential diagnosis of adnexal masses. Front Oncol 2022;12:968759.